



Article

# Properties of Ultra-High Molecular Weight Polyethylene Produced by Cyclic Impact Compaction and Reinforced with Graphene Nanoplatelets and Single-Walled Carbon Nanotubes

Alexandr Shtertser <sup>1,\*</sup> , Boris Zlobin <sup>1</sup>, Victor Kiselev <sup>1</sup>, Sergei Shemelin <sup>1</sup>, Vladislav Shikalov <sup>2</sup> , Evgenij Karpov <sup>1</sup> and Konstantin Ivanyuk <sup>1</sup>

<sup>1</sup> Lavrentyev Institute of Hydrodynamics, Siberian Branch of the Russian Academy of Sciences, Lavrentyev Ave. 15, 630090 Novosibirsk, Russia; zlobin.boris@mail.ru (B.Z.); vkiselev@ngs.ru (V.K.); s-shem@yandex.ru (S.S.); evkarpov@mail.ru (E.K.); kon.ivanyuk@gmail.com (K.I.)

<sup>2</sup> Khristianovich Institute of Theoretical and Applied Mechanics, Siberian Branch of the Russian Academy of Sciences, Institutskaya str., 4/1, 630090 Novosibirsk, Russia; v.shikalov@gmail.com

\* Correspondence: asterzer@mail.ru

**Abstract:** Polymer-based composites represent a special class of materials in demand by the industry. In comparison with other polymers, ultra-high molecular weight polyethylene (UHMWPE) is characterized by exceptionally high wear and impact resistance. There are different technologies for producing bulk material from UHMWPE powder and from its mixtures with various reinforcing additives. In this work, samples for research were made by cyclic impact compaction (CIC), graphene nanoplatelets and single-walled carbon nanotubes (SWCNTs) were the reinforcing nanofillers. Nanoscale detonation carbon (NDC) produced by the detonation decomposition of acetylene was employed as a graphene nanofiller. The obtained samples were subjected to a wear test, and their hardness and tensile strength were measured. Studies have shown that the reinforcement of UHMWPE with NDC and SWCNTs leads to an increase in its hardness by 6.4% and 19.6%, respectively. With the same nanofillers, the wear resistance when rubbing against a steel ball rises by 1.13 and 1.63 times, and the coefficient of friction drops by 10% and 20%, respectively. Meanwhile, the tensile strength of UHMWPE drops by 11.7% and 40.4%, and the elongation by 11.9% and 30.1% when reinforcing UHMWPE with NDC and SWCNTs, respectively.

**Keywords:** ultra-high molecular weight polyethylene; composite; nanoscale detonation carbon; single-walled carbon nanotubes; cyclic impact compaction; hardness; wear resistance; strength



**Citation:** Shtertser, A.; Zlobin, B.; Kiselev, V.; Shemelin, S.; Shikalov, V.; Karpov, E.; Ivanyuk, K. Properties of Ultra-High Molecular Weight Polyethylene Produced by Cyclic Impact Compaction and Reinforced with Graphene Nanoplatelets and Single-Walled Carbon Nanotubes. *J. Compos. Sci.* **2023**, *7*, 314. <https://doi.org/10.3390/jcs7080314>

Academic Editor: Francesco Tornabene

Received: 29 June 2023

Revised: 20 July 2023

Accepted: 28 July 2023

Published: 31 July 2023



**Copyright:** © 2023 by the authors. Licensee MDPI, Basel, Switzerland. This article is an open access article distributed under the terms and conditions of the Creative Commons Attribution (CC BY) license (<https://creativecommons.org/licenses/by/4.0/>).

## 1. Introduction

The ultra-high molecular weight polyethylene (UHMWPE) has a number of remarkable properties that make it suitable for a wide range of applications in industry and medicine. It is a proper material for manufacturing various parts of machines, mechanisms and devices, shoulder and hip implants and for defective bone replacement along with polytetrafluoroethylene (PTFE) [1–6]. UHMWPE is highly resistant to impact, so it is also used for protection against penetration by metallic projectiles, especially when it is reinforced with various additives and inserts [7–10].

UHMWPE was first synthesized in the last century, and its industrial production in powder form became possible based on the process of metal-complex catalysis of olefin polymerization developed in the 1950s by K. Ziegler and G. Natta [11,12]. Since the 1960s large-scale industrial production of bulk material from UHMWPE powder is based on methods of compression molding, ram extrusion, gel extrusion, spinning, etc. [1]. These technologies are complex and expensive, but they enable producing products of sufficiently large sizes. It is noteworthy that, in comparison with other polymers, the manufacture of bulk products from UHMWPE powder is associated with difficulties due to the high

viscosity of the melt (up to  $10^8$  Pa·s [13]) caused by the high molecular weight of this material (more than  $10^6$  g/mol) [14]. This required a significant modification of existing technologies for the production of thermoplastics to adapt them to UHMWPE [14–16]. The improvement of UHMWPE processing technologies continues even now [17–19]. Not so long ago, in 2007, a fundamentally new method for producing bulk material from UHMWPE powder was proposed, based on cyclic impact on the powder [20]. Later, the authors of this work gave this method the name cyclic impact compaction (CIC) and used it in the manufacture of compacts both from pure UHMWPE and with various additives and reinforcing metal inserts [10,21–23]. It should be emphasized that the peculiarity of UHMWPE is the presence of two structural phases in it, crystalline and amorphous. The density of the amorphous phase is  $0.855$  g/cm<sup>3</sup>, and the crystalline phase is  $0.999$  g/cm<sup>3</sup>. As noted in [20], the typical volume content of the crystalline phase in the initial powder is 60–75%. The production of bulk products using conventional technologies is usually accompanied by the melting of the polymer and subsequent solidification, after which the content of the crystalline phase decreases to about 50%. By the way, the melting point of UHMWPE is 132–138 °C [3], and the heating temperature in typical conventional sintering technologies is 180–220 °C [1]. As for the strength of the bulk material, it decreases with a decrease in the content of the crystalline phase. Therefore, it is desirable to avoid a noticeable drop in the content of the crystalline phase in the resulting bulk product. Apparently, the CIC technique has an advantage, since the powder is heated only to 100–120 °C before compaction [23] and the resulting material retains a high content of the crystalline phase of about 66% [21]. The processed material in the CIC procedure does not overheat, since the shock waves passing through the powder heat up and melt the particles only locally on their interfaces. As a result, the bonding of particles occurs without melting their entire volume. A detailed description of the mechanism of localization of deformation and heat release during pulsed loading of powder materials is given, e.g., in [24].

In order to improve certain operational properties of UHMWPE, as well as of other polymers, researchers and technologists use various additives, such as ultra-fine particles of hydroxyapatite, activated copper spinel, tungsten oxide, silicon carbide, basalt fibers, titanium oxide, silicon oxide, glass fibers, etc. [25–29]. Due to its high chemical inertness and biocompatibility, UHMWPE is actively used in modern medicine, where sometimes it is also necessary to improve its tribological, mechanical and other properties. In this regard, especially in the light of biocompatibility, various forms of carbon, such as graphene particles, carbon fibers, carbon nanotubes, etc., represent promising additives in the UHMWPE for medical applications [30].

The literature provides various, sometimes opposite, data on the effect of carbonaceous additives in UHMWPE. For example, in [31], due to the addition of graphene nanoparticles, it was possible to achieve a reduction in the coefficient of friction by 10% and an increase in hardness by 30% compared to pure UHMWPE. In [32], due to the addition of 10% carbon fibers to UHMWPE, the coefficient of friction was reduced by about 20%, but the wear resistance herewith fell by about 36%. Meanwhile, in [29], due to the addition of 0.5% carbon nanofibers, the friction coefficient of UHMWPE was reduced by half (from 0.1 to 0.05), and the wear resistance was increased by 2.7 times. Obviously, the tribological characteristics of the composite significantly depend on both the content and size of carbon fibers. In [16], fibers with a diameter of 7 microns and a length of 28 microns, and in [29] with a diameter of 60 nm and a length of 2 microns were used. The studies described in [33] have shown that the reinforcement of UHMWPE with carbon nanotubes (CNTs) leads to a decrease in its wear resistance. Both single-wall and multi-wall CNTs were used. In pin-on-disk tests, a layer of perfluoropolyether was applied to the surface of the UHMWPE as a lubricant. Based on the test results, the authors of [33] suggested that CNTs act as third abrasive body to increase wear once CNT is released from bulk polymer during friction. As well as tribological properties, the mechanical characteristics of UHMWPE are also sensitive to carbon additives. According to [34], due to the addition of 1% multi-walled carbon nanotubes (MWCNTs) to UHMWPE, the Young modulus of the

material increases by 1.4 times, and the yield stress by 1.5 times. Note that in [34], the tested material was prepared in a special way in the form of a thin (several microns thick) film. Again, in [35], it was shown that the addition of 0.5% carbon nanofibers to the polymer composite UHMWPE/HDPE leads to an increase in tensile strength by 32%. Let's add that in work [36], due to the addition of 1% MWCNTs to UHMWPE, its abrasive resistance was increased by 37%, the elongation increased by 2.4 times (from 290 to 700%) and the tensile strength decreased by 27% (from 30 to 22 MPa).

The objective of this work was to study the impact of nanofillers, such as single-walled carbon nanotubes (SWCNTs) and graphene nanoplatelets in the form of nanoscale detonation carbon (NDC), on the mechanical and tribological properties of the UHMWPE. The novelty of the work is that the properties of UHMWPE-based composites containing these nanofillers have not been studied before. The use of CIC technology to produce such composites is also a novelty to a certain extent.

## 2. Materials and Methods

Composite samples in the form of disks with a diameter of about 40 mm and a thickness in the range from 18 to 20 mm were made from mixtures of UHMWPE powder and carbonaceous additives by CIC technique described in detail in [21–23]. The method consists in applying a series of blows with a steel striker to the compacted material. The hydro-pneumatic device developed in LIH SB RAS enables striking the processed material with a frequency of  $9 \text{ s}^{-1}$  and an impact energy of up to 1 kJ. The number of strokes is several thousand and the total production time of the compact is several minutes. The device also enables applying a static force of 4 tons for prepressing the processed powder.

The main component of the initial powder mixtures was UHMWPE powder of the GUR 4120 brand (Ticona GmbH, Frankfurt, Germany) with a particle size of 120–140  $\mu\text{m}$  and molar mass of  $5 \cdot 10^6 \text{ g/mol}$ . One of the additives was NDC produced in LIH SB RAS, and the other additive was SWCNTs of the TUBALL™ brand kindly supplied by OCSiAl Company (Novosibirsk, Russia). NDC is a product of the decomposition of acetylene during its detonation in mixtures with oxygen at a low content of the latter. The method of NDC manufacture and its properties are described in detail in [37,38]. One of the features of the technology is that the morphology of NDC particles and their size depends on the oxygen content in the detonating mixture. The particles can be either rounded with a size of tens of nanometers or, with an increase in oxygen content, graphene-like with a size of 100–200 nm. In this work, we have used the NDC obtained as a result of detonation of an acetylene–oxygen mixture with an oxygen content of 42 vol.%. In this case, the NDC particles are multilayer graphene nanoplatelets with a thickness of about 20 nm and a length of 100–200 nm [37,38]. According to the OCSiAl certificate, carbon nanotubes of TUBALL™ brand have a diameter of  $1.46 \pm 0.02 \text{ nm}$  and a length of at least 5 microns. The product contains  $\geq 75\%$  nanotubes, 10% graphitized carbon and  $\leq 15\%$  iron in mass fractions.

For the manufacture of composite compacts, mixtures of UHMWPE + 0.5 wt.% NDC and UHMWPE + 0.5 wt.% SWCNTs were prepared. Since the properties of UHMWPE powder and applied nanofillers are very different, their mixing requires special approaches in order to get more or less homogeneous mixtures. Preparation of a mixture containing NDC was as follows. The required amount of UHMWPE powder was placed in a glass cup and then ethyl alcohol was added there so that the alcohol level was 5–10 mm higher than the powder level. Then the NDC powder was added to the cup and the composition was mixed manually with a wooden stick until a mass in the form of a thick liquid with a uniform color was obtained. After that, the cup with a mixture was kept in the oven at a temperature of 70 °C until the alcohol completely evaporates. In the case of SWCNTs, it turned out to be more difficult to prepare a homogeneous mixture. It was not possible to stir the composition manually to a homogeneous state, as in the case with NDC. Therefore, the powders were mixed using a blade rotated by a drilling machine with a rotation speed

of 1220 rpm. The blade of a special design with curved tips was fixed on a steel pin, which was inserted into the drill chuck, as shown in Figure 1.

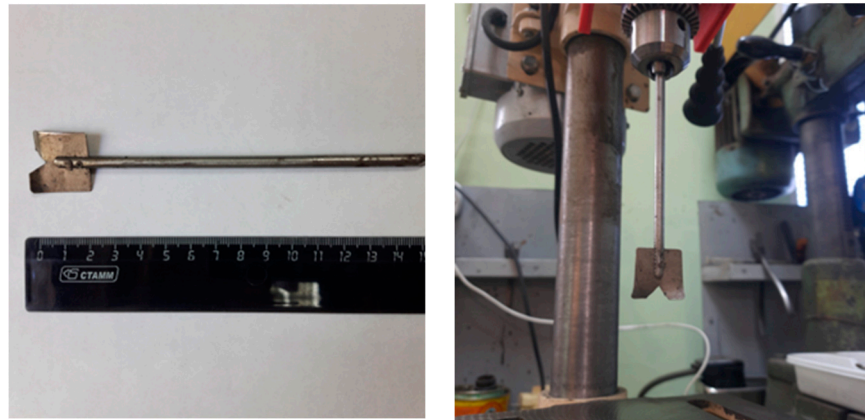


**Figure 1.** The blade on the pin (left) is inserted into the drill chuck (right).

Further, the blade was immersed in a glass jar with a liquid mass containing UHMWPE, SWCNTs and alcohol, and mixing was carried out for two hours. After that, the resulting liquid mass was placed in a thin layer in a flat dish and was kept for 7 h at a temperature of 70 °C until the alcohol completely evaporates. The powder mixtures made by the described methods were further compacted by the CIC technique. For comparative tests, compacts were also manufactured from pure UHMWPE. The procedure for making samples was as follows. The assembled mold filled with processed powder was kept in the oven at a temperature of 120 °C for 2.5 h. This time was required to warm up the mold with thick walls. Then CIC procedure was performed at an air pressure in the impact device of 10 bar, which corresponded to the energy of one blow of 655 J [23], and the compaction time was 200 s. Figure 2 as an example shows the view of the samples immediately after compaction. Samples made of pure UHMWPE are white, while composites with carbonaceous nanofillers are black.

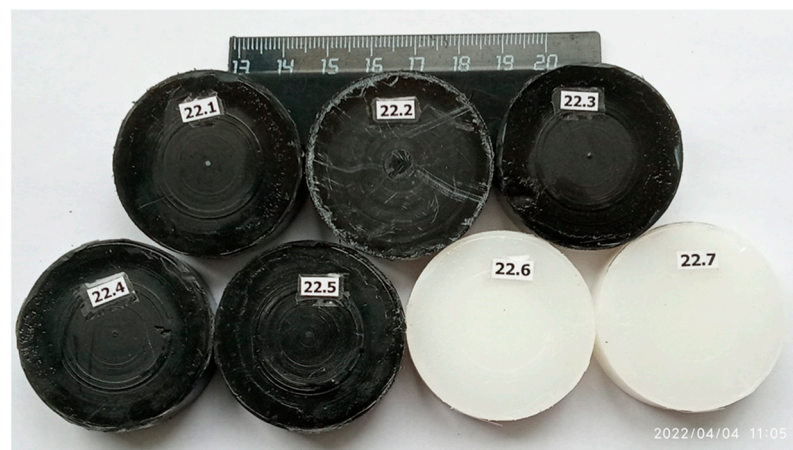


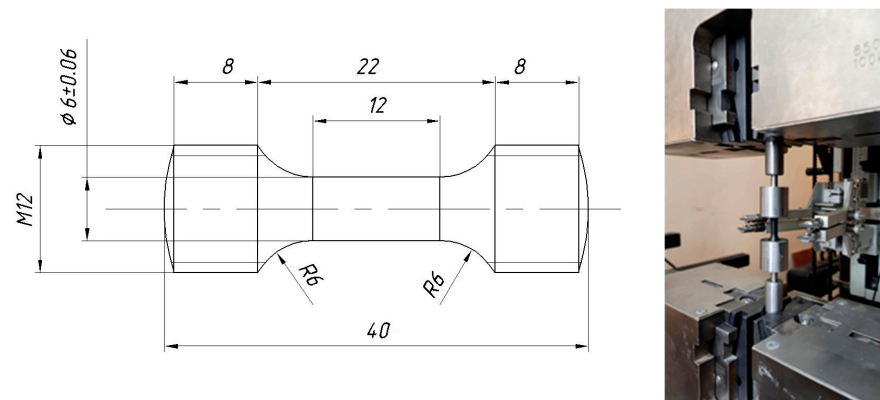
**Figure 2.** Disk-shaped compacts manufactured by the CIC technique from pure UHMWPE (white) and from UHMWPE with carbon nanofillers (black).

The parameters of produced samples are given in Table 1. Measurements of linear dimensions were made with a calliper, and mass measurements were made on the LV 210-A laboratory scales with an accuracy of 0.0005 g. Therefore, the volume and density of samples were determined with an accuracy not worse than 1%.

**Table 1.** Parameters of produced compacts.

Powder Composition	Sample Parameters				
	Diameter, mm	Height, mm	Mass, g	Volume, cm <sup>3</sup>	Density, g/cm <sup>3</sup>
UHMWPE	40.8 ± 0.1	18.3 ± 0.1	22.4 ± 0.0005	23.93 ± 0.12	0.94 ± 0.005
UHMWPE + 0.5 wt.% NDC	40.6 ± 0.1	17.9 ± 0.1	21.9 ± 0.0005	23.17 ± 0.12	0.95 ± 0.005
UHMWPE + 0.5 wt.% SWCNTs	40.7 ± 0.1	19.6 ± 0.1	24.3 ± 0.0005	25.50 ± 0.13	0.95 ± 0.005

Hardness of the produced samples was measured on the TU 2137 hardness tester (Tochpribor LLC, Ivanovo, Russia) in accordance with the Russian standard GOST 9012-59. Tensile testing of samples was carried out on a testing machine Zwick/Roell Z100 (Zwick GmbH & Co. KG, Ulm, Germany) according to the Russian standard GOST 11262-2017. The tensile rate was 10 mm/min. Figure 3 shows a tensile test specimen sketch, and a specimen itself cut out of a compact and placed in the clamps of a testing machine. Tribological tests were carried out on the UMT-2 device (Bruker, Karlsruhe, Germany) in the dry friction mode (ball-on-flat) with reciprocating motion. The counter body was a ball with a diameter of 6.35 mm made of structural ball-bearing steel. Images of the microstructure were obtained using an OLYMPUS GX-51 optical microscope (Olympus Corp., Tokyo, Japan) microscope and a Carl Zeiss Merlin VP Compact scanning electron microscope (Carl Zeiss AG, Oberkochen, Germany). The STRUERS Tegramin-20 sample preparation station (Denmark) was used to polish the samples before SEM examination. After polishing, the surface was covered with gold.

**Figure 3.** Drawing of a tensile test specimen (left) and the specimen in the clamps of a testing machine (right).

### 3. Results

Figure 4 shows the microstructure of produced compacts. As in previous studies [10,21–23], these experiments confirm that the CIC method enables producing dense compacts without cracks and delaminations.

In Brinell hardness measurements, the diameter of the ball was 5 mm, the load was 245.3 N and the holding time under load was 30 s. The measurements showed hardness values of  $59.8 \pm 1.8$ ,  $63.6 \pm 3.4$  and  $71.5 \pm 1.7$  for compacts made of pure UHMWPE, UHMWPE + 0.5 wt.% NDC and UHMWPE + 0.5 wt.% SWCNTs, respectively. Thus, reinforcement of UHMWPE with a small amount of NDC gives an increase in hardness by 6.3%, and the addition of carbon nanotubes increases the hardness by 19.6%. Table 2 shows the results of tensile testing of specimens. In these tests, on the contrary, maximal tensile strength and elongation has pure UHMWPE, and minimal values correspond to the composite with SWCNTs.

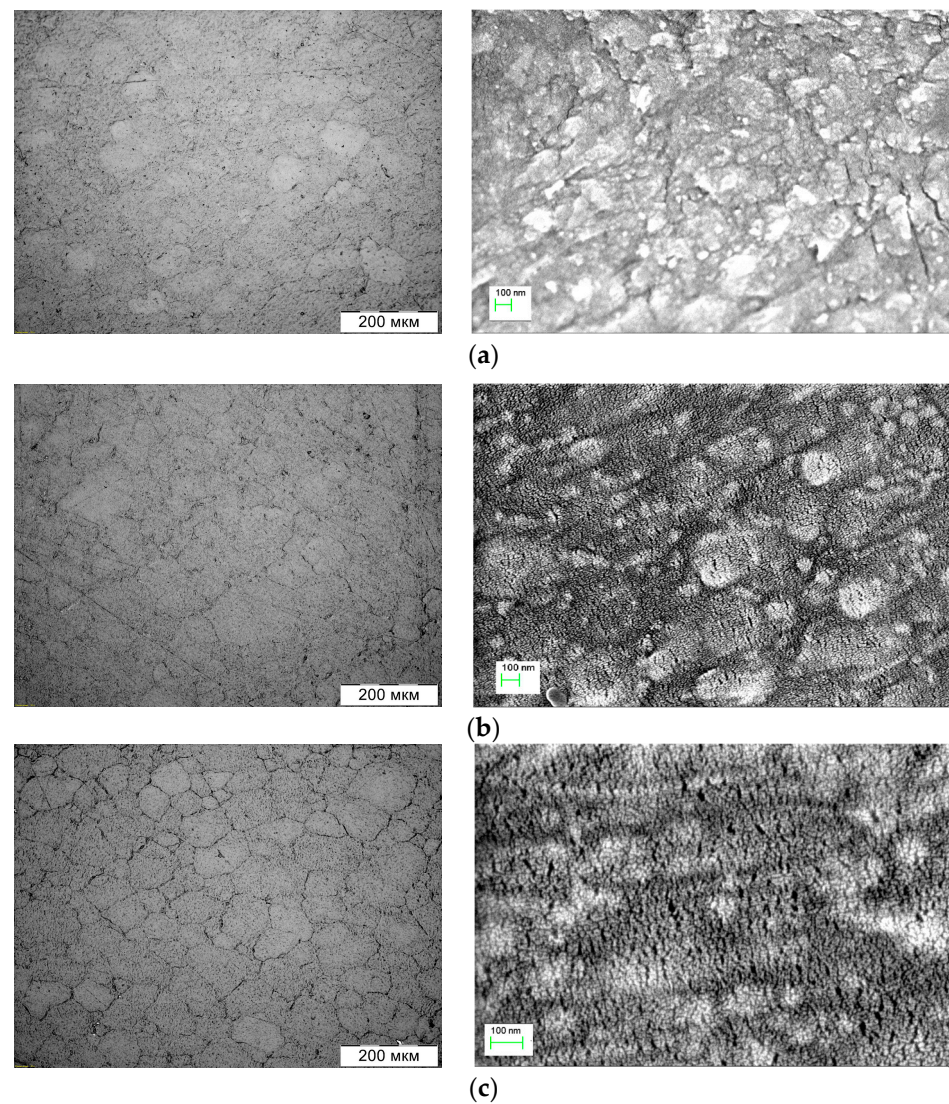


**Figure 4.** Microstructure of composites: (a) UHMWPE, (b) UHMWPE + 0.5 wt.% NDC and (c) UHMWPE + 0.5 wt.% SWCNTs. Optical (left) and SEM (right) images.

**Table 2.** Strength properties of the compacts:  $E$ —Young’s module,  $\sigma_{0.2}$ —elastic limit,  $\sigma_m$ —tensile strength,  $\delta$ —elongation.

Material	$E$ , MPa	$\sigma_{0.2}$ , MPa	$\sigma_m$ , MPa	$\delta$ , %
UHMWPE	$776.2 \pm 35.6$	$12.2 \pm 0.8$	$36.6 \pm 3.4$	$312 \pm 21$
UHMWPE + 0.5 wt.% NDC	$883.6 \pm 41.0$	$12.7 \pm 0.9$	$32.3 \pm 3.8$	$275 \pm 24$
UHMWPE + 0.5 wt.% SWCNTs	$767.9 \pm 37.3$	$12.3 \pm 1.0$	$21.8 \pm 2.2$	$218 \pm 22$

Figure 5 shows typical stress–strain diagrams of produced materials. Obviously, the diagrams of a pure polymer and a composite containing NDC have a similar appearance. At the same time, the diagram of a composite containing SWCNTs differs in the absence of hardening during deformation. It is noteworthy that the diagram for a composite with a NDC passes slightly higher than the other two, up to the destruction of this composite. In our opinion, this indicates the presence of interface bonds at the contacts of NDC particles and polymer matrix in this composite. The reasoning for this issue is given below in the Discussion section.

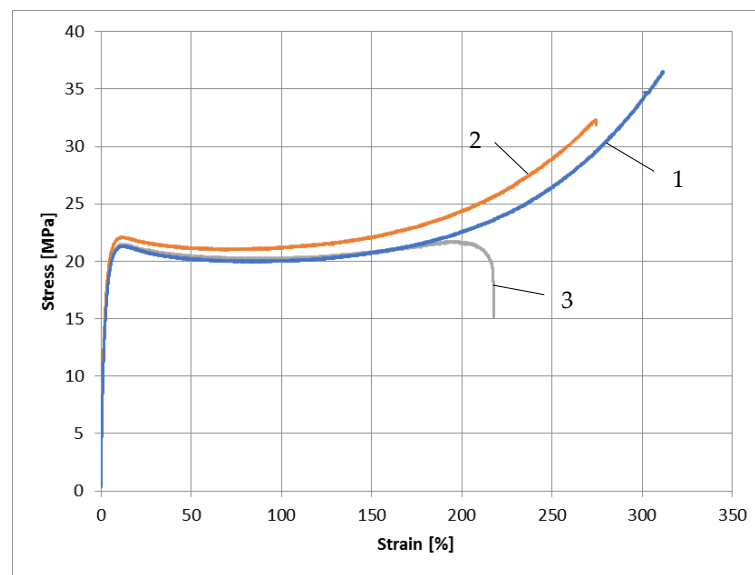


**Figure 5.** Stress–strain diagrams of (1) UHMWPE, (2) UHMWPE + 0.5 wt.% NDC, (3) UHMWPE + 0.5 wt.% SWCNTs.

In dry friction wear tests, a steel ball with a diameter of 6.35 mm performed a reciprocating slide on the surface of the test sample with an amplitude of 5 mm and a frequency of 5 Hz. The load on the ball was 25 N, the test duration was 2000 s and the friction path was 100 m. Table 3 shows the test results.

**Table 3.** The results of testing the produced materials for wear.

Material	Wear, mm <sup>3</sup>	Coefficient of Friction
UHMWPE	0.052 ± 0.006	0.10 ± 0.01
UHMWPE + 0.5 wt.% NDC	0.046 ± 0.005	0.09 ± 0.01
UHMWPE + 0.5 wt.% SWCNTs	0.032 ± 0.004	0.08 ± 0.01

## 4. Discussion

### 4.1. Changes in Mechanical and Tribological Properties

The conducted studies show that nanofillers used improve some properties of UHMWPE, but not all. Adding 0.5 wt.% NDC leads to a rise in polymer hardness by 6.4%, a decrease in wear (ball-on-flat test) by 11.5% and a drop in the coefficient of friction by 10%. The addition of SWCNTs to the polymer leads to an even higher improvement in hardness and tribological parameters. Thus, hardness rises by 19.6%, wear drops by 38.5% and the coefficient of friction drops by 20%. As for the mechanical properties under tension, we have different results for different parameters. With the addition of NDC, the Young's modulus of the polymer rises by 13.8%, and with the addition of SWCNTs, it practically does not change. The elastic limit  $\sigma_{0.2}$  also practically does not change with the introduction of both NDC and SWCNTs. However, both nanofillers lead to a significant reduction in the tensile strength  $\sigma_m$  and elongation  $\delta$  of the polymer. Furthermore, the addition of NDC leads to a smaller drop in these characteristics than the addition of SWCNTs. As Table 2 shows, a polymer with NDC in comparison with pure UHMWPE has a strength lower by 11.7% and elongation by 11.9%. And, the polymer with SWCNTs has the same parameters reduced, respectively, by 40.4% and 30.1%. For greater clarity, Table 4 shows changes in the mechanical and tribological characteristics of UHMWPE when it is modified by addition of NDC and SWCNTs. The plus and minus signs mean, respectively, the rise and drop of the values as a percentage in relation to the corresponding parameters of compacts made from pure UHMWPE. Evidently, both carbonaceous nanofillers used in this work lead to an

improvement in the tribological properties of UHMWPE, but at the same time, its strength and plasticity degrade.

**Table 4.** Changes (in percent) in the mechanical and tribological parameters of UHMWPE when reinforcing it with nano additives: HB—Brinell hardness,  $E$ —Young’s module,  $\sigma_m$ —tensile strength,  $\delta$ —elongation,  $W$ —wear and COF—coefficient of friction.

Additive	HB	$E$	$\sigma_m$	$\delta$	$W$	COF
NDC	+6.4	+13.8	−11.7	−11.9	−11.5	−10.0
SWCNTs	+19.6	-	−40.4	−30.1	−38.5	−20.0

Note: a decrease in wear by 11.5% and 38.5% corresponds to an increase in wear resistance by 1.13 and 1.63 times, respectively.

Interestingly, the stress–strain curves of pure UHMWPE and a composite with NDC have a hardening section, and a composite with SWCNTs does not show hardening. Note that the diagram for a composite with a NDC passes slightly higher than the other two, up to the destruction of this composite. Evidently, the type of stress–strain diagram is determined not only by the content of the reinforcing component but also by the adhesion at the contacts of nanoparticles with the polymer matrix (interface bonding). It is quite logical to assume that for a composite with formed adhesion, the stress–strain curve should pass higher than in the absence of adhesion. The reasoning for this issue is given below. Also note, that curves 1 and 2 in Figure 5 are similar to stress–strain diagrams presented in [28] and inherent in pure UHMWPE and UHMWPE-based composites containing glass fibers.

The results of this work to some extent coincide with the data from [31,36] regarding the rise in hardness and wear resistance and reducing the coefficient of friction and tensile strength due to the addition of graphene nanoparticles and multilayer carbon nanotubes to UHMWPE. Evidently, the increase in the hardness and wear resistance of UHMWPE due to mentioned nano additives is associated with the high rigidity and strength of graphene-like nanoparticles and carbon nanotubes. For example, as shown in [39,40], the Young’s modulus of graphene reaches 920 GPa and carbon nanotubes reaches 950 GPa with a tensile strength of 63 GPa. The drop in the tensile strength, in our opinion, can be explained by a lower adhesion at the polymer–nanoparticle interface compared with the strength of the polymer itself. However, in order to understand the mechanism of failure of the considered composites under mechanical load, additional research is required.

#### 4.2. Theoretical Considerations

In our opinion, the strength characteristics of the composite largely depend on the adhesion at the nanoparticle–polymer matrix interface. It is noteworthy that adhesion can be affected, e.g., by any pretreatment of the material added to the polymer. In particular, in [28], it was shown that the pretreatment of glass fibers with a KH-550 silane coupling agent improves the mechanical and tribological properties of the composite by increasing the mentioned adhesion. In this example, the adhesion is due to the formation of  $\text{SiCH}_2$  and  $\text{Si}(\text{CH}_3)_2$  compounds at the glass–polymer interface. In our case, adhesion can be determined by the formation of C–C bonds between the carbon atoms of nanofillers and polymer. However, since hydroxyl and carbonate groups are present on the surface of graphene nanoplatelets [38], they can impair the above-mentioned adhesion. Generally speaking, the change in the mechanical properties of the polymer may depend not only on the said adhesion but may also be associated with a change in the microstructure of the polymer under the influence of nanofillers. For example, in [27], it is stated that nanoparticles lead to grain grinding in the polymer.

Let’s evaluate the effect of nano additives on the strength properties of UHMWPE in terms of the presence or absence of the said adhesion. To do this, we will consider the polymer incompressible so that during deformation there is no change in the volume of the sample, only its shape changes. The reason lies in the value of the polymer’s Poisson’s ratio, which is 0.46 [41] and is close to the value of 0.5 for an incompressible material.



The deformation behavior of the polymer matrix is associated with the presence of two phases—amorphous and crystalline. At the initial stage of deformation, the plastic flow is localized in the amorphous phase, since its strength is lower than the strength of the crystalline one. With a gradual increase in deformation, randomly oriented crystalline lamellae begin to rearrange into a more oriented structure with alternating amorphous and crystalline phases, and then the lamellae also begin to deform [42,43]. Such a deformation mechanism determines the type of stress–strain diagrams 1 and 2 shown in Figure 5. Carbon nanoparticles are supposed to be incompressible and non-deformable, since the strength of graphene and carbon nanotubes far exceeds the strength of the polymer matrix.

First, we need to find the volume fractions of NDC and SWCNTs for a given mass content of 0.5%. Let  $m_1$  and  $m_2$  denote the mass fractions of the components in the composite,  $v_1$  and  $v_2$  are the volume fractions and  $\rho_1$  and  $\rho_2$  are the densities. The numbers 1 and 2 refer to the polymer and the additive, respectively. Then the relationship between volume and mass fractions is expressed by the formulas  $v_1 = (m_1/\rho_1)/[(m_1/\rho_1) + (m_2/\rho_2)]$  and  $v_2 = (m_2/\rho_2)/[(m_1/\rho_1) + (m_2/\rho_2)]$ . The density of NDC particles is equal to the density of graphite 2.2 g/cm<sup>3</sup>. As for SWCNTs, they are hollow inside and their density averaged over the volume is less than the density of graphite. Considering the diameter of SWCNT is 1.46 nm and the wall thickness is 0.35 nm, it is easy to find the average density, which is 1.6 g/cm<sup>3</sup>. Then, the calculation according to the above formula for  $v_2$  gives a volume content of 0.2 and 0.3% for NDC and SWCNTs, respectively. Further, it follows from geometric considerations that for the volume fraction of any component  $v$ , the linear fraction of this component, i.e., its content along an arbitrary line drawn in the volume of the composite, will be  $v_2^{1/3}$ . Similarly, the surface fraction of the component in any section of the composite is  $v_2^{2/3}$ .

Next, we argue as follows. Let there be no adhesion at the nanoparticle–polymer interface. Then, when the sample is stretched, the fraction of its area in the cross-section equal to  $v_2^{2/3}$  does not resist stretching and the entire load falls on the fraction of the area of  $(1 - v_2^{2/3})$ . The entire load falls on the polymer component with an increase in the actual stress by  $1/(1 - v_2^{2/3})$  times. Accordingly, the strength and modulus of elasticity of the composite should decrease by  $1/(1 - v_2^{2/3})$  times compared to polymer without additives. Now let there be an adhesion at the nanoparticle–polymer interface, and the adhesion value is  $\sigma_a$ . Then, when the sample is stretched, the load is distributed over its entire cross-section. With an increase in the load up to  $\sigma_a$ , since we consider nano additives to be non-deformable, only the polymer component is deformed, the linear fraction of which is  $(1 - v_2^{1/3})$ . That is, with the same load, the elongation of the composite will be  $1/(1 - v_2^{1/3})$  times less than the elongation of a sample made of pure polymer. Accordingly, the Young's modulus of the composite will be  $1/(1 - v_2^{1/3})$  times greater than that of a pure polymer. With further stretching, if  $\sigma_a$  is equal to or exceeds the strength of the polymer, destruction will occur at a load equal to the strength of the polymer. If  $\sigma_a$  is less than the strength of the polymer, then at some stage of stretching, when the stress in the material reaches  $\sigma_a$ , the nanoparticle–polymer bonds will collapse and further deformation will proceed according to the scenario described above for the case of lack of adhesion. As a result, the sample will break at a stress  $1/(1 - v_2^{2/3})$  times less than the strength of the polymer. Similar arguments about elongation  $\delta$  lead to the conclusion that in the absence of adhesion, it should be the same for both the composite and the pure polymer. However, if the adhesion is equal to or exceeds the strength of the polymer, then the elongation of the composite should be  $1/(1 - v_2^{1/3})$  times less.

Table 5 shows the values of the mechanical parameters of composites calculated according to the described theoretical model considering the presence or absence of adhesion at the nanoparticle–polymer interface.

**Table 5.** Calculated values of mechanical properties of composites:  $E$ —Young's modulus,  $\sigma$ —tensile strength and  $\delta$ —elongation.

Additive	Mass Fraction, %	Density, g/cm <sup>3</sup>	Volume Fraction, %	Adhesion			No Adhesion		
				$E$ , MPa	$\sigma$ , MPa	$\delta$ , %	$E$ , MPa	$\sigma$ , MPa	$\delta$ , %
NDC	0.5	2.2	0.2	888.1	36.6	273	763.9	36.0	312
SWCNTs	0.5	1.6	0.3	907.0	36.6	267	760.0	35.8	312

A comparison of the data from Tables 3 and 5 shows a good coincidence of the experimental and calculated values of the Young's modulus and elongation for a composite with NDC if we assume the presence of a strong interfacial during the process of deformation until the beginning of the composite fracture. However, the theoretical tensile strength exceeds the experimental one by about 10%, when considering the loss of adhesion before the sample fracture. Generally speaking, such a difference is often associated with the spread of measured values of mechanical parameters for different samples of the same material. For a composite with SWCNTs, we can state a good coincidence of the calculated (in the absence of adhesion) and experimental values only for the Young's modulus. For the remaining parameters (strength and elongation), the experimental values are significantly lower than the theoretical ones. Thus, the proposed computational model predicts quite well the mechanical properties of a composite reinforced with graphene nanoparticles and only with respect to the Young's modulus for a composite reinforced with carbon nanotubes. Evidently, the considered simplified model is not quite suitable for reinforcing particles with high values of aspect ratio when one size of the particle significantly exceeds the other two sizes, which is typical for nanotubes and nanofibers. Obviously, the proposal needs to be improved taking into account the shape of the reinforcing particles. The most effective way to study the effect of the size, shape, volume content and orientation of additives on the properties of the composite is modern computer modeling, such as described in [44]. In addition, it is necessary to take into account the effect of additives on the properties of the polymer itself, but more research is needed to study this effect in detail.

As for the improvement of the tribological properties of the polymer due to the nano additives considered, in our opinion, this effect is solely related to the high strength of NDC and SWCNT. Usually, the process of wear during friction is accompanied by a number of processes, including pulling hard inclusions out of the soft matrix. Due to the elongated shape of nanotubes and nanofibers, it is much harder to pull them out of the polymer than graphene particles. Therefore, a composite with SWCNTs demonstrates significantly higher wear resistance than a composite with NDC.

## 5. Conclusions

Composites based on UHMWPE with reinforcing nano additives in the form of NDC and SWCNTs were manufactured by the CIC technique using a laboratory hydro-pneumatic impact device. Studies have shown that the reinforcement of UHMWPE with an additive of 0.5 wt.%, NDC and SWCNTs lead to a rise in its hardness, respectively, by 6.4% and 19.6%, a rise in wear resistance by 1.13 and 1.63 times and a drop in the coefficient of friction by 10% and 20%. Meanwhile, the tensile strength under the influence of said nano additives drops by 11.7% and 40.4% and plasticity by 11.9% and 30.1%, respectively. Thus, SWCNTs have an advantage over NDC in rising the hardness of the polymer and improving its tribological parameters. But at the same time, SWCNTs worsen the strength and ductility of UHMWPE to a greater extent than NDC. To evaluate the mechanical properties of polymer-based composites with reinforcing nano additives, a physical model is proposed considering the interfacial adhesion. It is preferable to employ the obtained composite materials when it is necessary to increase the wear resistance of UHMWPE in dry friction conditions and there are no strict requirements for the mechanical strength of the material.

**Author Contributions:** Conceptualization, A.S. and B.Z.; methodology, A.S. and B.Z.; investigation, V.K., S.S., V.S., E.K. and K.I.; resources, B.Z.; writing—original draft preparation, V.K.; writing—review and editing, A.S.; supervision, B.Z.; project administration, A.S.; funding acquisition, A.S. and B.Z. All authors have read and agreed to the published version of the manuscript.

**Funding:** This research was funded by the Ministry of Science and Higher Education of the Russian Federation, project 121121700104-0.

**Institutional Review Board Statement:** Not applicable.

**Informed Consent Statement:** Not applicable.

**Data Availability Statement:** Not applicable.

**Acknowledgments:** The authors express their gratitude to OCSiAl Company (Novosibirsk, Russia) for kindly providing SWCNTs for experiments. The study was conducted at the Equipment Sharing Center “Mechanics” of LIH SB RAS and ITAM SB RAS.

**Conflicts of Interest:** The authors declare no conflict of interest.

## References

1. Kelly, J.M. Ultra-High Molecular Weight Polyethylene. *J. Macromol. Sci. Polym. Rev.* **2002**, *42*, 355–371. [[CrossRef](#)]
2. Sobieraj, M.C.; Rinnac, C.M. Ultra high molecular weight polyethylene: Mechanics, morphology, and clinical behavior. *J. Mech. Behav. Biomed.* **2009**, *2*, 433–443. [[CrossRef](#)] [[PubMed](#)]
3. Hussain, M.; Naqvi, R.A.; Abbas, N.; Khan, S.M.; Nawaz, S.; Hussain, A.; Zahra, N.; Khalid, M.W. Ultra-High-Molecular-Weight-Polyethylene (UHMWPE) as a Promising Polymer Material for Biomedical Applications: A Concise Review. *Polymers* **2020**, *12*, 323. [[CrossRef](#)] [[PubMed](#)]
4. Ammarullah, M.I.; Afif, I.Y.; Maula, M.I.; Winarni, T.I.; Tauviqirrahman, M.; Jamari, J. Tresca stress evaluation of Metal-on-UHMWPE total hip arthroplasty during peak loading from normal walking activity. *Mater. Today Proc.* **2022**, *63*, 143–146. [[CrossRef](#)]
5. Sentra, M.R.; Marques, M.F.V. Synthetic Polymeric Materials for Bone Replacement. *J. Compos. Sci.* **2020**, *4*, 191. [[CrossRef](#)]
6. Shah, Q.M.Z.; Kowser, M.A.; Chowdhury, M.A.; Chani, M.T.S.; Alamry, K.A.; Hossain, N.; Rahman, M. Modeling Fracture Formation, Behavior and Mechanics of Polymeric Materials: A Biomedical Implant Perspective. *J. Compos. Sci.* **2022**, *6*, 31. [[CrossRef](#)]
7. Chricker, R.; Mustacchi, S.; Massarwa, E.; Eliasi, R.; Aboudi, J.; Haj-Ali, R. Ballistic Penetration Analysis of Soft Laminated Composites Using Sublaminar Mesoscale Modeling. *J. Compos. Sci.* **2021**, *5*, 21. [[CrossRef](#)]
8. Shen, Y.; Wang, Y.; Yan, Z.; Cheng, X.; Fan, Q.; Wang, F.; Miao, C. Experimental and Numerical Investigation of the Effect of Projectile Nose Shape on the Deformation and Energy Dissipation Mechanisms of the Ultra-High Molecular Weight Polyethylene (UHMWPE) Composite. *Materials* **2021**, *14*, 4208. [[CrossRef](#)]
9. Dasgupta, K. Role of carbon nanotubes in the ballistic properties of boron carbide/carbon nanotube/ultrahigh molecular weight polyethylene composite armor. *Ceram. Int.* **2020**, *46*, 4137–4141. [[CrossRef](#)]
10. Shtertser, A.A.; Zlobin, B.S.; Kiselev, V.V.; Shemelin, S.D.; Bukatnikov, P.A. Characteristics of Reinforced Ultra-High Molecular Weight Polyethylene during Its Ballistic Penetration. *J. Appl. Mech. Tech. Phys.* **2020**, *61*, 471–478. [[CrossRef](#)]
11. Ziegler, K.; Breil, H.; Holzkamp, E.; Martin, H. Verfahren zur Herstellung von hochmolekularen Polyäthylenen. DE Patent 973,626, 14 April 1960.
12. Natta, G. Stereospezifische Katalysen und isotaktische Polymere. *Angew. Chem.* **1956**, *68*, 393–403. [[CrossRef](#)]
13. Li, Y.; He, H.; Ma, Y.; Geng, Y.; Tan, J. Rheological and mechanical properties of ultrahigh molecular weight polyethylene/high density polyethylene/polyethylene glycol blends. *Adv. Ind. Eng. Polym. Res.* **2019**, *2*, 51–60. [[CrossRef](#)]
14. Truss, R.W.; Han, K.S.; Wallage, J.F.; Geil, P.H. Cold Compaction Molding and Sintering of Ultra High Molecular Weight Polyethylene. *Polym. Eng. Sci.* **1980**, *20*, 747–755. [[CrossRef](#)]
15. Kulkarni, K.M. High-Pressure Non-Isothermal Processing of Linear Polyethylenes. *Polym. Eng. Sci.* **1976**, *16*, 15–24. [[CrossRef](#)]
16. Lupton, J.M.; Regester, W. Exceptionally Rigid and Tough Ultrahigh Molecular Weight Linear Polyethylene. U.S. Patent 3,944,536, 16 March 1976.
17. Gaspar-Cunha, A.; Covas, J.A.; Sikora, J. Optimization of Polymer Processing: A Review (Part I—Extrusion). *Materials* **2022**, *15*, 384. [[CrossRef](#)]
18. Gaspar-Cunha, A.; Covas, J.A.; Sikora, J. Optimization of Polymer Processing: A Review (Part II—Molding Technologies). *Materials* **2022**, *15*, 1138. [[CrossRef](#)]
19. Yilmaz, G.; Ellingham, T.; Turng, L.-S. Injection and injection compression molding of ultra-high-molecular weight polyethylene powder. *Polym. Eng. Sci.* **2019**, *59*, E170–E179. [[CrossRef](#)]
20. Jauffres, D.; Lame, O.; Vigier, G.; Dore, F. Microstructural origin of physical and mechanical properties of ultra high molecular weight polyethylene processed by high velocity compaction. *Polymer* **2007**, *48*, 6374–6383. [[CrossRef](#)]

21. Zlobin, B.S.; Shtertser, A.A.; Kiselev, V.V.; Shemelin, S.D.; Poluboyarov, V.A.; Zhdanok, A.A. Cyclic Impact Compaction of Ultra High Molecular Weight Polyethylene Powder. *J. Appl. Mech. Tech. Phys.* **2017**, *58*, 435–442. [[CrossRef](#)]
22. Zlobin, B.S.; Shtertser, A.A.; Kiselev, V.V.; Shemelin, S.D. Impact Compaction of Ultra High Molecular Weight Polyethylene. *J. Phys. Conf. Ser.* **2017**, *894*, 012091. [[CrossRef](#)]
23. Shtertser, A.; Zlobin, B.; Kiselev, V.; Shemelin, S.; Ukhina, A.; Dudina, D. Cyclic Impact Compaction of an Ultra High Molecular Weight Polyethylene (UHMWPE) Powder and Properties of the Compacts. *Materials* **2022**, *15*, 6706. [[CrossRef](#)] [[PubMed](#)]
24. Nesterenko, V.F. *Dynamics of Heterogeneous Materials*, 1st ed.; Springer Science+Business Media: New York, NY, USA, 2001; ISBN 978-1-4419-2926-6.
25. Selyutin, G.E.; Gavrilov, Y.Y.; Voskresenskaya, E.N.; Zakharov, V.A.; Nikitin, V.E.; Poluboyarov, V.A. Composite Materials Based on Ultra High Molecular Weight Polyethylene: Properties, Application Prospects. *Chem. Sustain. Dev.* **2010**, *18*, 375–388.
26. Gogoleva, O.V.; Petrova, P.N.; Popov, S.N.; Okhlopkova, A.A. Wear-resistant composite materials based on ultrahigh molecular weight polyethylene and basalt fibers. *J. Frict. Wear* **2015**, *36*, 301–305. [[CrossRef](#)]
27. Poluboyarov, V.A.; Korotaeva, Z.A.; Pauli, I.A.; Zhdanok, A.A.; Selyutin, G.E. Modification of Polymers by Nanodispersed Ceramic Particles. *Chem. Sustain. Dev.* **2014**, *22*, 385–392.
28. Panin, S.V.; Kornienko, L.A.; Huang, Q.; Buslovich, D.G.; Bochkareva, S.A.; Alexenko, V.O.; Panov, I.L.; Berto, F. Effect of Adhesion on Mechanical and Tribological Properties of Glass Fiber Composites, Based on Ultra-High Molecular Weight Polyethylene Powders with Various Initial Particle Sizes. *Materials* **2020**, *13*, 1602. [[CrossRef](#)] [[PubMed](#)]
29. Panin, S.V.; Kornienko, L.A.; Alexenko, V.O.; Buslovich, D.G.; Bochkareva, S.A.; Lyukshin, B.A. Increasing Wear Resistance of UHMWPE by Loading Enforcing Carbon Fibers: Effect of Irreversible and Elastic Deformation, Friction Heating, and Filler Size. *Materials* **2020**, *13*, 338. [[CrossRef](#)]
30. Puértolas, J.A.; Kurtz, S.M. Evaluation of carbon nanotubes and graphene as reinforcements for UHMWPE-based composites in arthroplastic applications: A review. *J. Mech. Behav. Biomed.* **2014**, *39*, 129–145. [[CrossRef](#)]
31. Chih, A.; Anson-Casaos, A.; Puertolas, J.A. Frictional and mechanical behaviour of graphene/UHMWPE composite coatings. *Tribol. Int.* **2017**, *116*, 295–302. [[CrossRef](#)]
32. Wang, Y.; Yin, Z.; Li, H.; Gao, G.; Zhang, X. Friction and wear characteristics of ultrahigh molecular weight polyethylene (UHMWPE) composites containing glass fibers and carbon fibers under dry and water-lubricated conditions. *Wear* **2017**, *380–381*, 42–51. [[CrossRef](#)]
33. Liu, Y.; Sinha, S.K. Wear performances and wear mechanism study of bulk UHMWPE composites with nacre and CNT fillers and PFPE overcoat. *Wear* **2013**, *300*, 44–54. [[CrossRef](#)]
34. Ruan, S.L.; Gao, P.; Yang, X.G.; Yu, T.X. Toughening high performance ultrahigh molecular weight polyethylene using multiwalled carbon nanotubes. *Polymer* **2003**, *44*, 5643–5654. [[CrossRef](#)]
35. Sui, G.; Zhong, W.H.; Ren, X.; Wang, X.Q.; Yang, X.P. Structure, mechanical properties and friction behavior of UHMWPE/HDPE/carbon nanofibers. *Mater. Chem. Phys.* **2009**, *115*, 404–412. [[CrossRef](#)]
36. Markevich, I.A.; Selyutin, G.E.; Drokin, N.A.; Selyutin, A.G. Electrical and Mechanical Properties of the High-Permittivity Ultra-High-Molecular-Weight Polyethylene-Based Composite Modified by Carbon Nanotubes. *Tech. Phys.* **2020**, *65*, 1106–1113. [[CrossRef](#)]
37. Shtertser, A.A.; Ulianitsky, V.Y.; Batraev, I.S.; Rybin, I.S. Production of Nanoscale Detonation Carbon using a Pulse Gas-Detonation Device. *Tech. Phys. Lett.* **2018**, *44*, 395–397. [[CrossRef](#)]
38. Shtertser, A.A.; Rybin, D.K.; Ulianitsky, V.Y.; Park, W.; Datekyu, M.; Wada, T.; Kato, H. Characterization of Nanoscale Detonation Carbon Produced in a Pulse Gas-Detonation Device. *Diam. Relat. Mater.* **2020**, *101*, 107553. [[CrossRef](#)]
39. Yu, M.-F.; Lourie, O.; Dyer, M.J.; Moloni, K.; Kelly, T.F.; Ruoff, R.S. Multiwalled Carbon Nanotubes Under Tensile Load. *Science* **2000**, *287*, 637–640. [[CrossRef](#)]
40. Poot, M.; van der Zant, H.S.J. Nanomechanical properties of few-layer graphene membranes. *Appl. Phys. Lett.* **2008**, *92*, 063111. [[CrossRef](#)]
41. Bergstrom, J.S.; Kurtza, S.M.; Rinnac, C.M.; Edidin, A.A. Constitutive modeling of ultra-high molecular weight polyethylene under large-deformation and cyclic loading conditions. *Biomaterials* **2002**, *23*, 2329–2343. [[CrossRef](#)]
42. Danilova, S.N.; Okoneshnikova, A.V.; Okhlopkova, A.A. Polymer materials based on ultra-high molecular weight polyethylene: Structure and properties. *Arct. Subarct. Nat. Resour.* **2022**, *27*, 631–642. (In Russian) [[CrossRef](#)]
43. Galeski, A.; Bartczak, Z.; Vozniak, A.; Pawlak, A.; Walkenhorst, R. Morphology and Plastic Yielding of Ultrahigh Molecular Weight Polyethylene. *Macromolecules* **2020**, *53*, 6063–6077. [[CrossRef](#)]
44. Rouway, M.; Nachtane, M.; Tarfaoui, M.; Chakhchaoui, N.; Omari, L.E.H.; Fraija, F.; Cherkaoui, O. Mechanical Properties of a Biocomposite Based on Carbon Nanotube and Graphene Nanoplatelet Reinforced Polymers: Analytical and Numerical Study. *J. Compos. Sci.* **2021**, *5*, 234. [[CrossRef](#)]

**Disclaimer/Publisher's Note:** The statements, opinions and data contained in all publications are solely those of the individual author(s) and contributor(s) and not of MDPI and/or the editor(s). MDPI and/or the editor(s) disclaim responsibility for any injury to people or property resulting from any ideas, methods, instructions or products referred to in the content.